Bullard et al., The Molecular Elasticity of the Insect Flight Muscle Proteins Projectin and Kettin

Supporting text

Cloning and expression of projectin and kettin fragments: Projectin sequences coding for PIg24 to PIg26 (accession number AF047475) was obtained by PCR using *Drosophila* genomic DNA. The corresponding protein sequence is from VPVTGEPLPSKD at the N-terminus to TANSVTISWKPP at the C-terminus, with a molecular weight of 80 kDa. The DNA was subcloned into the pETM11 expression vector, which has a 6His tag at the N-terminus, and the vector was transformed into *E. coli* BL21(DE3)pRARE cells (Stratagene). Expressed protein from a 2 l culture was in inclusion bodies. The inclusion body pellet was washed with 50 mM K-phosphate pH 7.5, 0.1% Triton X-100, 2 mM DTT and then taken up in 10 ml 8 M urea, 50 mM Na-phosphate pH 7.5. The soluble fraction was dialyzed against 50% glycerol, 20 mM Tris pH 8.0, 1 mM DTT, 1 mM EDTA, then against the same buffer with 25% glycerol and 50 mM NaCl, and finally against this buffer without glycerol. At each stage, insoluble protein was removed by centrifugation.

Kettin sequence coding for KIg17 to KIg21 (accession number AJ245406) was cloned and expressed by the same method as used for the projectin fragment. The sequence at the N-terminus of the protein is DAPISPPHFTAE and at the C-terminus is TSGTLKCTGGKT; the molecular weight is 71 kDa. The protein was expressed in *E. coli* BL21(DE3)pJY2 cells (Stratagene); soluble protein was purified from the cell lysate on a (Ni-NTA)-agarose column (Qiagen) and then on a Mono-Q column (Pharmacia). A construct coding for three Ig domains in the Sls sequence upstream of kettin (SIg4 to SIg6) (accession number AJ544075) was obtained by PCR. The corresponding protein sequence is from SDSEMASDIEPI at the N-terminus to FLNIRGSGLPAS at the C-terminus, with a molecular weight of 38 kDa. The construct was subcloned into the pET8c vector and expressed and purified by the same method as used for KIg17-KIg21. The kettin fragment KIg34/35 was cloned and expressed as described by Kulke et al. (2001; ref 1). Proteins were concentrated with a Millipore centrifugal concentrator.

AFM. To study the mechanical properties of kettin and projectin we used a home-built single molecule atomic force microscope (AFM). The spring constant of each individual cantilever (MSCT-AUHW: sharpened silicon nitride gold-coated cantilevers; Veeco Metrology Group, Santa Barbara, CA) was calibrated using the equipartition theorem (2) and varied between 20-80 pN/nm depending on the type of cantilever. With this system it is possible to measure the force as a function of the extension of the protein (force-extension mode), or measure the elongation of the protein at a constant force (force-feedback mode). The step time response of our force-feedback system was ~20 ms. Unless noted in the text, the pulling speed of all force–extension curves was in the range of 0.4–0.6 nm/ms.

Single protein recordings. In a typical experiment, a small aliquot of the purified protein (~10-50 µl, 10 µg/ml) was allowed to adsorb to a clean glass coverslip (for ~10min) and then rinsed with PBS pH 7.4. Segments of the proteins were then picked up randomly by adsorption to the cantilever tip, by pressing it down onto the sample for 1-2 seconds at forces of several nanonewtons, and stretched for several hundred nanometers. The probability of picking up a protein was typically kept low (less than one in 50 attempts) by controlling the amount of protein used to prepare the coverslips. In order to study the effect of low temperature on refolding kinetics we used a simple device where we enclosed the AFM inside a refrigerator, filled with lead bricks (to increase the heat capacity). We then turned on the refrigerator and let the AFM equilibrate at low temperatures (7-10^{o}C). After ~1h the power was turned off because the mechanical noise introduced by the cooling system interferes with the AFM measurements. The temperature increase was typically very slow (~8^{o}C/hr) during the duration of the experiment (20-30 min).

Analysis of force extension curves. The elasticity of the stretched proteins was analyzed using the worm-like chain (WLC) model of polymer elasticity (3, 4):

$$\mathrm{F}(x) = \frac{kT}{p}\left[\frac{1}{4}\left(1-\frac{x}{Lc}\right)^{-2} - \frac{1}{4} + \frac{x}{Lc}\right] \qquad \text{(eq. S1)}$$

where *F* is force, *p* is the persistence length, *x* is end-to-end length, *Lc* is contour length of the stretched protein, *k* is Boltzmann's constant, and *T* is absolute temperature. The adjustable parameters are the persistence length, (which defines the flexibility), and the contour length. The change in contour length was used to calculate the size of the folded domain.

Estimation of the unfolding rate from force-ramp experiments. In order to analyze the data of Fig. 4B and 4D quantitatively, we used a simple two-state kinetic model for mechanical unfolding (5, 6). In this model, a protein is exposed to a force that increases linearly with time, simulating the conditions of our force-ramp experiment. According to this model the cumulative probability, Pu(F), that an unfolding event has occurred at a force lower than or equal to F, is given by:

$$\mathrm{P_u}(F) = 1 - e^{-\frac{\alpha_o}{a}\int_0^F e^{\frac{f\cdot\Delta x_u}{kT}}df} \qquad \text{(eq. S2)}$$

where *a* is the rate of change of the applied force (*a* = 200 pN/s in our experiments), α_0 is the rate of unfolding at zero force, Δx_u is the distance to the transition state and the other symbols have their usual meaning. For the kettin fragment, KIg17-KIg21, values of $\alpha_0 = 8 \times 10^{-3}$ s^{-1} and $\Delta x_u = 0.17$ nm readily describe the data (continuous line, Fig. 4D). In the case of native projectin we used an equation that describes the cumulative probability of the unfolding of two independent populations of domains with different unfolding rates, α_{o1} and α_{o2} (7):

$$\mathrm{P_u}(F) = 2 - e^{-\frac{\alpha_{o1}}{a}\int_0^F e^{\frac{f\cdot\Delta x_{u1}}{kT}}df} - e^{-\frac{\alpha_{o2}}{a}\int_0^F e^{\frac{f\cdot\Delta x_{u2}}{kT}}df} \qquad \text{(eq. S3)}$$

Using this equation we estimate: $\alpha_{o1} = 0.3 \times 10^{-3}$ s^{-1} and $\alpha_{o2} = 7 \times 10^{-2}$ s^{-1} using a $\Delta x_{u1} = 0.2$ nm and $\Delta x_{u2} = 0.1$ nm (solid line in Fig. 4B).

Estimation of the refolding distance using a three pulse protocol. Determination of the folding distance, Δx_f, involves measuring how much the folding rate constant depends on the applied force. To measure the folding distance, we used a three pulse protocol (8) to first

completely unfold and extend the protein and obtain the contour length of the unfolded protein, Lc. Then the protein was rapidly relaxed to a length Lo for a fixed period of time (10 s). A second extension then allowed us to count the number of domains that refolded during the relaxation period at that particular length, L_o. From this plot we can estimate how the applied force affects the refolding rate (8). In the experiment shown in Fig. 5C the protein is allowed to fold under an applied force that depends on the ratio L_0/Lc. Hence we can write:

$$\frac{N_{\text{refolded}}}{N_{\text{total}}} = 1 - e^{-tk_f^o(\text{Lo/Lc})} \qquad \text{(eq. S4)}$$

where $k_f(L_0/Lc)=k_f^0\exp(-F(L_o/Lc)\Delta x_f/kT)$. Since during a refolding experiment the contour length, Lc, is known, we can calculate the force, $F(L_0/Lc)$, that strains the protein at length L_o using the WLC equation.

Monte Carlo simulations. The folding/unfolding of a domain was modeled as a two state Markovian process where the probability of unfolding was $P_u=N_f*\alpha*\Delta t$ where N_f is the number of folded domains and Δt is the polling interval (8-11). The folding probability was $P_f=N_u*\beta*\Delta t$ where N_u is the number of unfolded domains. The rate constants for unfolding, α, and refolding, β, are given by $\alpha=\alpha_o\exp(F\Delta x_u/kT)$ and $\beta=\beta_o\exp(-F\Delta x_f/kT)$ where F is the applied force and Δx_u and Δx_f are the unfolding and folding distances.

Additional Data

a) Cantilever Drift

An important problem in force-clamp experiments like those shown in Fig 6 and Fig S2, is cantilever drift and this can lead to significant errors in the force measurements. We found a small fraction (about 1 in 20) of cantilevers had exceptionally low drift and we used these for force-clamp experiments. Figure S1 shows the measurement of the drift from 4 different cantilevers (n=21 measurements; Kc: 30-35 pN/nm). As shown by Figure S1A the drift over ~ 1 min is in general quite random; some cantilevers tend to have negative or positive slope with random fluctuations. However, on average the drift during the first 60 s tends to have a positive slope of 0.17 pN/s (Fig S1B); hence after 60 sec the cantilever would have drifted on average by ~ 10 pN. This effect would certainly affect the force the protein is subjected to at very long time scales (> 1 min).

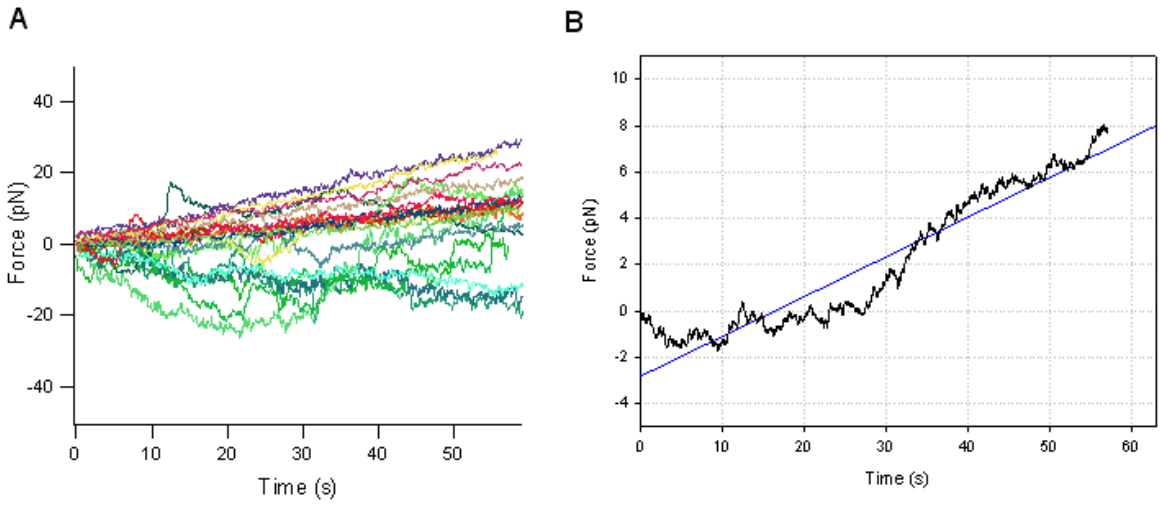

Figure S1. Measurement of cantilever drift. A) Force as a function of time for 4 different cantilevers (n=21 measurements; Kc: 30-35 pN/nm). B) Average cantilever drift; the slope of the force vs. time plot is 0.17 pN/nm.

As discussed by Fernandez and Li (12), one way to independently measure the actual value of the quenched force is to measure the magnitude of the elastic recoil observed immediately after relaxing to unfolded polypeptide chain to the lower force. Since we know the length of

the unfolded chain, we used the worm-like-chain equation to estimate the actual force after initial relaxation. We have used this method to estimate the force after relaxation in Fig 6 and in Fig S2.

b) Additional Force-clamp data

Figure S2 shows additional examples of force clamp data obtained on a longer time scale (> 1 min) than those shown in Fig 6. In Fig. S2A, a projectin molecule was first unfolded and extended at a high force (95 pN). We observed 1 step and then 6 steps (because of the compressed time scale these are seen as one large step) corresponding to the unfolding of 7 domains. There was an initial large step elongation of ~200 nm upon application of force. (This initial phase most likely corresponds to the length of the folded polypeptide chain plus a few already unfolded domains.) Then the protein was relaxed to a force of 35 pN; before the protein reached its fully collapsed state there was a dramatic increase in the noise level with length fluctuations of up to 50 nm peak-to-peak. Three phases are distinguishable: i) a fast phase (<100ms) corresponding to the elastic recoil of the unfolded polypeptide chain and accounting for ~20% of the unfolded length of the protein; ii) a slow phase (~5 nm/s) characterized by large fluctuations in end-to-end length (up to 50nm); and iii) again a fast phase (350nm/s) that corresponds to the final collapse of the polypeptide chain to its folded length.

In the experiment shown in Fig. S2B the protein was first unfolded and extended at 68 pN (8 unfolding steps preceded by a large elongation of ~120 nm; see inset on the left) and then the force was dropped to ~5 pN; the polypeptide chain is seen to quickly (270nm/s) contract to its original end-to-end length. After 6 s a force of 68 pN was applied again (marked by arrow) and we observed 4 steps indicating that during this time 4 out of 8 domains were able to refold under force. Then the force was lowered to 38 pN and we observed the polypeptide chain collapsing in fast and very slow (here, 4.5 nm/s) phases.

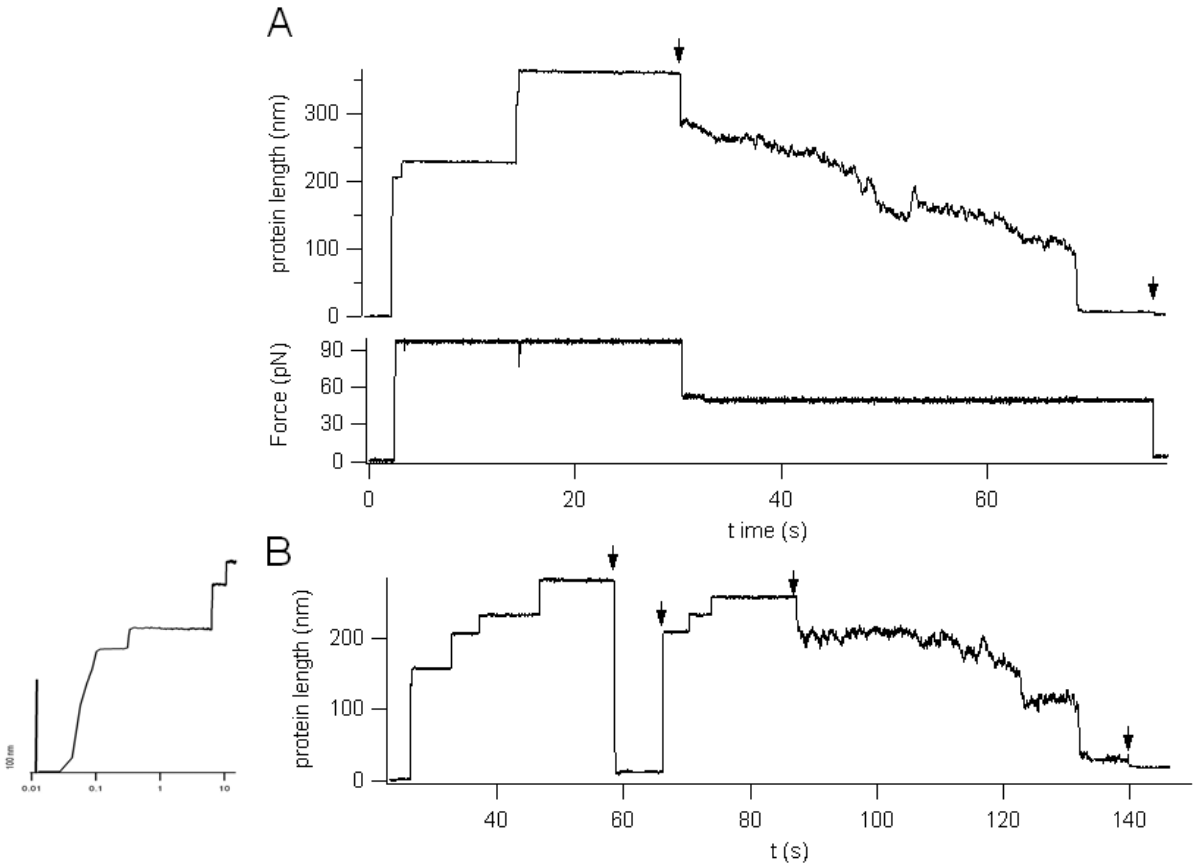

Figure S2. Additional collapse trajectories of unfolded projectin domains under force. We used force-clamp AFM to examine the effect of a mechanical force on the folding of projectin domains. A) A projectin molecule was first unfolded and extended at a high force (95 pN). We observe several steps corresponding to the unfolding of 7 domains. Then the protein was relaxed to a force of 35 pN (calculated from the WLC equation) and then to 15pN. B) A projectin molecule was extended at 68 pN (8 unfolding steps) and then the force was dropped to ~5 pN (marked by arrow); after 6 s the force was stepped to 73 pN (4 steps are detected) and after ~15 s then the force was lowered to 38 pN and finally to 0 pN. The inset shows the initial response to a stretching force in a log time scale.

c) Effect of temperature on unfolding forces

Figure S3 shows unfolding force histograms obtained at 26°C (red trace) and 14°C (blue trace). The mean unfolding forces are 97.4 ± 36.7 pN at 14°C and 74.7 ± 38.9 pN at 26°C. Hence lowering the temperature by ~10°C increases the unfolding forces by ~23 pN. This translates into a Q_{10} for unfolding of 1.3. In contrast the Q_{10} for refolding is almost twice as large (Q_{10} = 2.5).

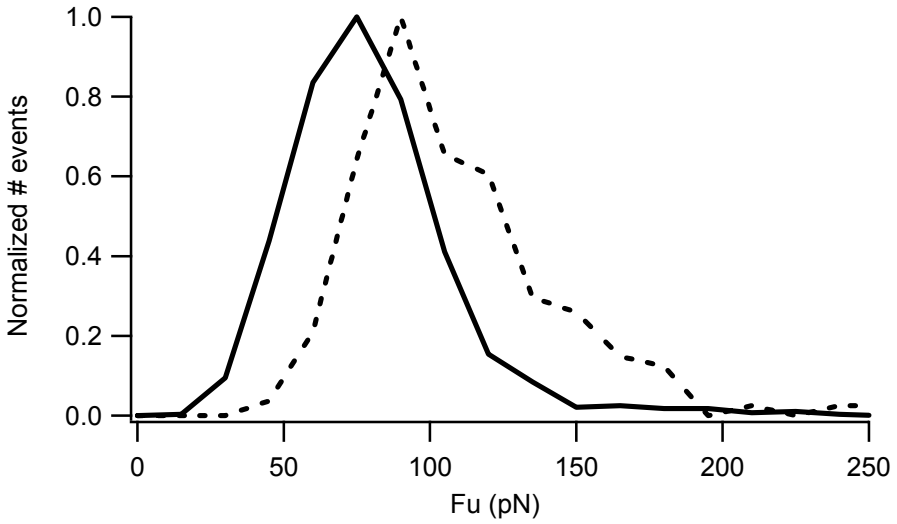

Figure S3. Effect of temperature on projectin domain unfolding forces. Normalized unfolding force histograms obtained at 26°C (continuous trace) and 14°C (dashed trace). The mean unfolding forces are 97.4 ± 36.7 pN (n=328) at 14°C and 74.7 ± 38.9 pN at 26°C (n=846). These data where obtained using the same cantilever.

d) Refolding of projectin domains.

Figure S4 shows a typical experiment in which a single projectin molecule remained attached to an AFM tip allowing for repeated extension and relaxation cycles (up to 28 cycles in this experiment over a period of ~9 min). After each extension, the molecule was allowed to relax completely (the relaxation traces are not shown). In this experiment we waited 15 s between each stretching pulse. Consecutive force-extension curves display similar patterns, demonstrating that domain unfolding is fully reversible and that projectin domains can

undergo multiple cycles of extension/relaxation with no signs of molecular fatigue or rundown.

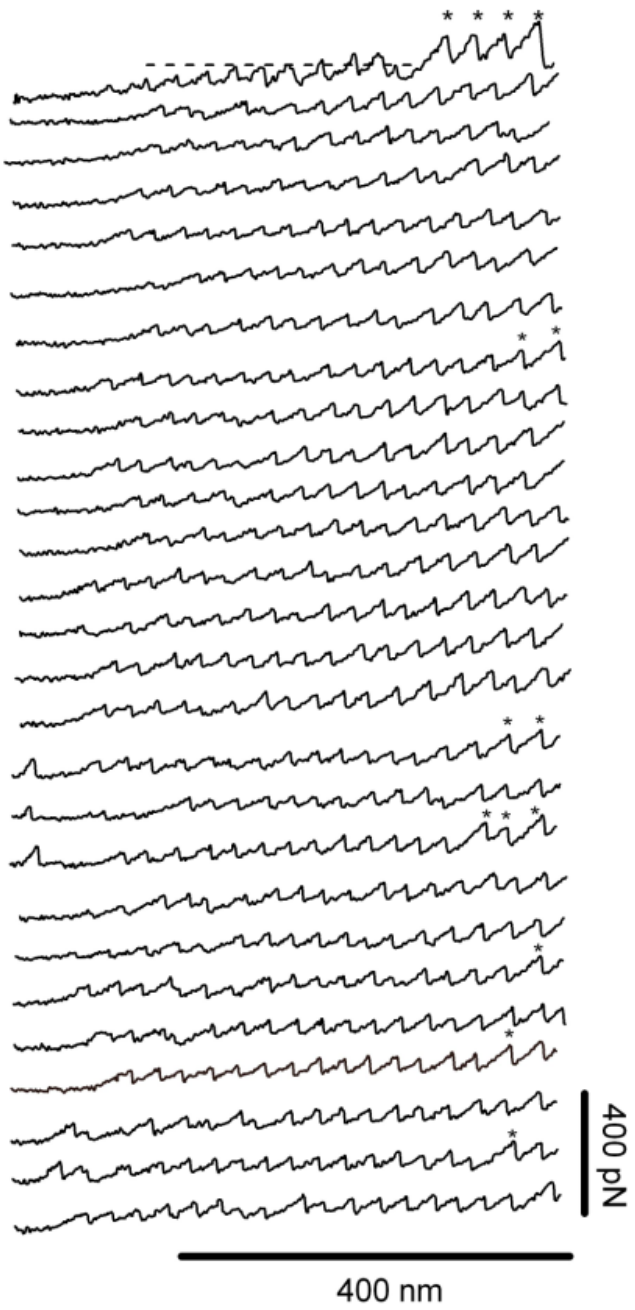

Figure S4. The refolding of projectin domains is very robust. A series of force curves collected from a single molecule over approximately 9 minutes. The "high-force' peaks are marked by an asterisk.

References

1. Kulke, M., C. Neagoe, B. Kolmerer, A. Minajeva, H. Hinssen, B. Bullard, and W.A. Linke. (2001). *J. Cell Biol.* 154:1045-1057.
2. Florin, E.L., Rief, M., Lehmann, H., Ludwig, M., Dornmair, C., Moy, V.T., and Gaub, H.E. (1995). *Biosen. Bioelectr*. **10**, 895
3. Marko, J.F., and E.D. Siggia. (1995). *Macromolecules.* 28:8759-8770.
4. Bustamante, C., Marko, J.F., Siggia, E.D. & Smith, S. (1994). *Science* **265**, 1599–1600
5. Oberhauser, A.F., P.K. Hansma, M. Carrion-Vazquez, and J.M. Fernandez. (2001). *Proc. Natl. Acad. Sci. USA.* 98:468-472.
6. Schlierf, M., H. Li, and J.M. Fernandez. (2004). *Proc. Natl. Acad. Sci.* 101:7299-7304.
7. Hukkanen, E.J., Wieland, J.A., Gewirth, A., Leckband, D.E., Braatz, R.D. (2005) *Biophys J.* 89(5):3434-45
8. Carrion-Vazquez, M., A.F. Oberhauser, S.B. Fowler, P.E. Marszalek, S.E. Broedel, J. Clarke, and J.M. Fernandez. 1999. *Proc. Natl. Acad. Sci. USA.* 3694-3699.
9. Rief, M., M. Gautel, F. Oesterhelt, J.M. Fernandez, and H.E. Gaub. (1997). *Science.* 276:1109-1112.
10. Oberhauser, A.F., P.E. Marszalek, H.P. Erickson, and J.M. Fernandez. (1998). *Nature*. 393:181-185.
11. Kellermayer, M.S.Z., S.B. Smith, H.L. Granzier, and C. Bustamante. (1997). *Science.* 276:1112-1116.
12. Fernandez, J.M., and H. Li. (2004). *Science.* 303:1674-1678.